Arch. Metall. Mater., Vol. 61 (2016), No 2, p. 577–580

DOI: 10.1515/amm-2016-0098

K. NIESPODZIANA*#, K. JURCZYK**, M. JURCZYK*

SYNTHESIS OF NITI BASED NANOCOMPOSITES REINFORCED BY HA ADDITION

NiTi alloy is well known for its unique properties, such as good ductility at room temperature, good corrosion resistance and also thermal shape memory effects. On the other hand hydroxyapatite has a combination of desirable properties, such as low density and excellent compatibility with the bone which used as ceramic reinforced phases can change the properties and thermal stability of the NiTi alloy.

In this study, the NiTi alloy matrix shape memory composite reinforced by hydroxyapatite particles was successfully fabricated using mechanical alloying and powder metallurgical process. The structural evaluation of milled and heat treated powders was studied by X-ray diffraction, scanning electron microscopy and transmission electron microscopy. The differential scanning calorimetry was used to measure the phase transformation temperatures. The porosity, Vickers' hardness and corrosion resistance of the TiNi-HA composites were investigated. The results show that the increase of the weight ratio of hydroxyapatite causes increase the porosity and decrease the corrosion resistance. The fabricated NiTi alloy matrix composite possesses lower density and higher Vickers' hardness as the pure NiTi shape memory alloy, yet still exhibiting the shape memory effect.

Keywords: biomaterial, NiTi, hydroxyapatite, nanocomposite, mechanical alloying

1. Introduction

Researchers have exhibited an increased interest in exploring numerous biomedical applications of nanomaterials and nanocomposites [1, 2]. Till now, it has been shown that implants made from metallic, carbon, or oxide bionanomaterials considerably improved the prosthesis strength and their biocompatibility. Fabrication technique including mechanical alloying (MA) of elemental powder mixtures have been used for synthesis of nanocrystalline alloys [3].

NiTi alloy is important for orthopedic implant applications and hard-tissue replacements based on shape memory and super-elasticity effects [4]. The shape memory effect observed this alloy is due to the martensitic transformation from B2–CsCl structure to a low-density monoclinic B19' structure. The high nickel content of the NiTi alloys might result in potentially negative effects on the surrounding tissue by inducing allergic responses [5]. One of the methods that allow the change of biological properties of NiTi alloys is the modification of its chemical composition. The other way is to produce a composite that will exhibit the favorable mechanical properties of NiTi and excellent biocompatibility and bioactivity of ceramic. The most commonly used ceramic employed in medicine is hydroxyapatite (HA). The ceramic coating on the titanium improves the surface bioactivity but often flakes off as a result of poor ceramic/metal interface bonding, which may cause the surgery to fail. For this reason, composite materials containing titanium and ceramic as a reinforced phase are expected to have broad practical applications [6]. Recently, the NiTi alloy matrix shape memory composite reinforced by nano-sized SiC particles was successfully fabricated [7]. The fabricated NiTi composite possesses lower density, higher storage modulus and almost the same equivalent strength as the dense NiTi shape memory alloy.

In this work, mechanical alloying and powder metallurgical process were used to prepare nanocrystalline NiTi-x wt.% HA composites (x = 0, 2.5, 5, 10). Structure, mechanical, corrosion properties and the martensitic transformation were investigated. To the best of our knowledge, there are no reports on HA addition to properties of NiTi alloy.

2. Materials and methods

NiTi-x wt.% HA nanocomposites were prepared by MA and annealing process (x=0, 2.5, 5 and 10). Elemental powders were weighted, blended and poured into vials in glove box (Labmaster 130) filled with automatically controlled argon atmosphere ($O_2 \leq 2$ ppm and $H_2O \leq 1$ ppm). A composition of a starting materials mixture was corresponding to a stoichiometry of the "ideal" reaction. MA was performed using SPEX 8000 Mixer Mills. Reaction atmosphere was argon. A round bottom stainless vials were used. The weight ratio of hard steel balls to mixed powder equaled 10:1. MA process in both cases lasted 10 hours. Obtained amorphous, as-milled materials were heat treated at 800 ^{o}C for 0.5 h under high purity argon to form cubic structure crystallizing in a CsCl-type structure. Materials were produced using elements in powder form (Ni: 3-7 μm, Ti:

* POZNAN UNIVERSITY OF TECHNOLOGY, INSTITUTE OF MATERIALS SCIENCE AND ENGINEERING, 5 M. SKLODOWSKA-CURIE STR., 60-965 POZNAN, POLAND

** POZNAN UNIVERSITY OF MEDICAL SCIENCES, DEPARTMENT OF CONSERVATIVE DENTISTRY AND PERIODONTOLOGY, 70 BUKOWSKA STR., 60-812 POZNAN, POLAND

Corresponding author: katarzyna.niespodziana@put.poznan.pl

≤45 μm; Alfa Aesar and HA: ≤50 μm; Sigma–Aldrich). Purity of starting metallic elements was at least 99.9 wt.%.

The porosity of the fabricated samples was measured by the relative density method. Structure, microstructure, composition and morphology of materials were studied by X-ray diffraction (XRD), scanning electron microscopy (SEM) and transmission electron microscopy (TEM). XRD data of studied alloy and composites were obtained from Panalytical Empyrean with Cu Kα (λ=1.54056 Å). This method was used to study structure of prepared TiNi alloy and TiNi-HA nanocomposites milled for different time. XRD data were used to calculate average crystallite size by using Scherrer equation. Microstructure and elements composition of obtained powders were determined using an SEM associated with energy dispersive spectroscopy (EDS). The martensitic transformation of the samples was analyzed using a differential scanning calorimeter (Q200,TA) with a heating/cooling rate of 5 °C/min. Corrosion resistance behavior was examined during potentiodynamic tests in Ringer solution with scanning range and speed -2.5 to 2 V and 1 mV/s, respectively, on Solatron 1285 potentiostat.

3. Results and discussion

The behavior of MA process was studied by X-ray diffraction and microstructural investigations. Fig. 1 shows a series of XRD spectra of mechanically alloyed Ni-Ti-2.5 wt.% HA powder mixture (55.07 wt.% Ni, 44.93 wt.% Ti) subjected to milling for increasing time. The originally sharp diffraction lines of Ni and Ti gradually become broader and their intensity decreases with milling time (not shown). The powder mixtures milled for 10 h have transformed completely to the amorphous phase, without formation of an other phases (Fig. 1d). During the MA process the crystalline size of the titanium decreases with MA time and reaches a steady value of about 35 nm after 10 h of milling. This size of crystallites seems to be favourable to the formation of an amorphous phase, which develops at the Ni-Ti interfaces. Formation of the nanocrystalline NiTi alloy was achieved by annealing the amorphous material in high purity argon atmosphere at 800 °C for 0.5 h (Fig. 1e). Except CsCl-type structure (B2) with cell parameter a = 3.018 Å other phases such as B19', $NiTi_2$ and Ni_3Ti are detected. When HA is added to NiTi-x wt.% HA the lattice constant a increases.

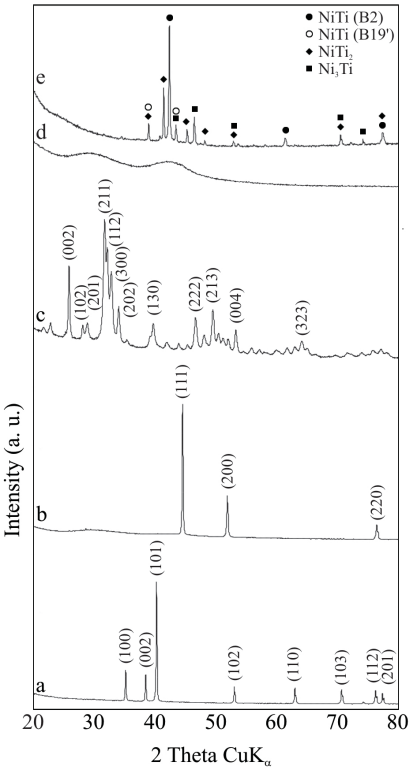

Fig. 1. XRD spectra of a mixture of Ti (a), Ni (b) and HA (c) powders mechanically alloyed for 10 h (d) and after annealing 800 °C/0.5 h (e)

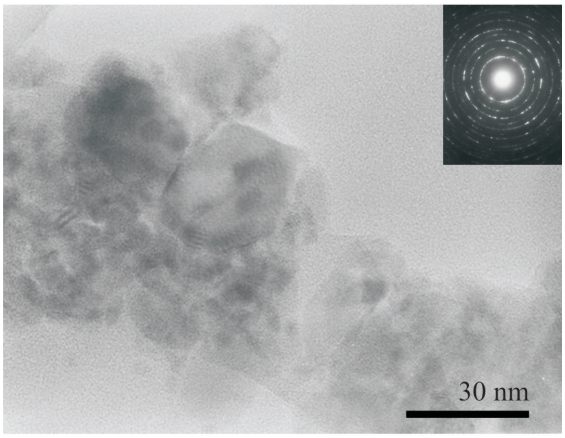

Fig. 2. TEM micrograph and electron diffraction pattern (insets) of the milled and annealed NiTi sample

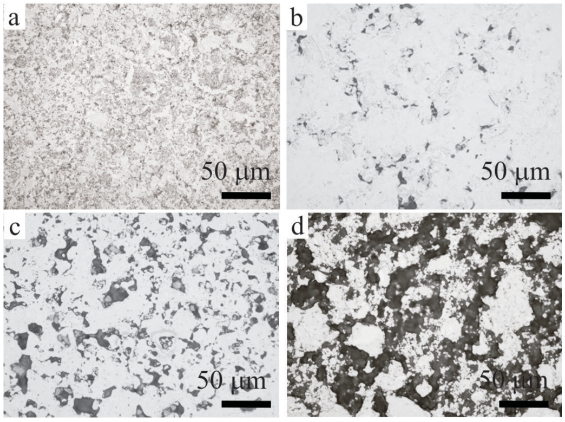

Fig. 3. Optical micrographs of the nanostructured NiTi alloy (a), NiTi-2.5 wt. % HA (b), NiTi-5 wt. % HA (c) and NiTi-10 wt.% HA (d) nanocomposites

Microstructure and possible local ordering in the NiTi samples was studied by TEM. The sample milled for 10 h was mostly amorphous as appears from a high resolution image (not shown). Microstructure of the annealed NiTi sample is shown in Fig. 2. Analysis of high resolution images revealed the presence of well developed crystallites with broad range of sizes from 4 up to more than 30 nm. SAED pattern obtained from large area (200 μm) contains sharp rings corresponding to NiTi alloy with CsCl structure.

The Vickers microhardness of the sintered nanocomposites exhibit various distribution corresponding to constitutional change and increase with the rise of HA contents. Reinforced by HA particles, the Vickers hardness of NiTi-2.5 wt.% HA composite (890 HV0.3) is higher than that of nanostructured NiTi alloy (650 HV0.3). This effect is directly connected with structure refinement and obtaining of nanostructure. The change of the chemical compositions of NiTi-x wt.% HA nanocomposites leads also to a distribution of the properties. With the increase of the HA contents in NiTi nanocomposite increase of porosity is noticeable (Fig. 3). A porous structure can significantly reduce the Young's modulus of studied nanocomposities.

The polarization curves of NiTi-x wt.% HA nanocomposites are shown in Fig. 4. The polarization data obtained for sintered composites, including corrosion potentials (E_C) and corrosion current densities (I_C) are summarized in Table I. From this table it is possible to observe that hydroxyapatite doped to NiTi had a negative effect on corrosion resistance of NiTi. The result indicated that there was no significant difference in corrosion resistance among NiTi-2.5 wt.% HA (I_C = 2.6×10^{-6} Acm^{-2}, E_C =−0.667 V vs. SCE) and NiTi-5 wt.% HA (I_C = 3.2×10^{-6} Acm^{-2}, E_C =−0.972 V vs. SCE) although there was a significant difference in porosity (see Fig. 3). The corrosion test results indicate that the nanostructured NiTi-10 wt.% HA composite possesses lower corrosion resistance and thus higher corrosion current density (I_C = 5.2×10^{-5} Acm^{-2}) in Ringer's solutions. The corrosion potential (E_C) of NiTi-2.5 wt.% HA sample shifted to the nobler direction.

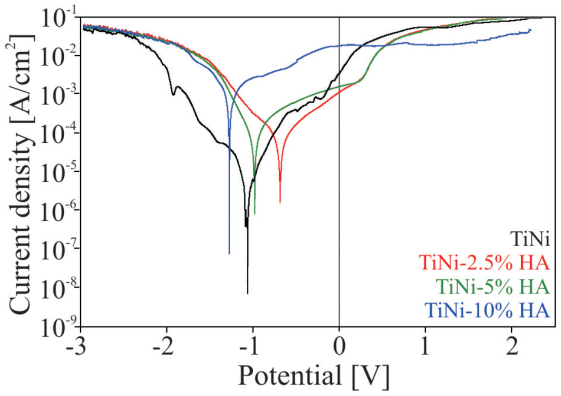

Fig. 4. Potentiodynamic polarization curves of studied bulk NiTi-type nanomaterials in Ringer's solution at 37 °C

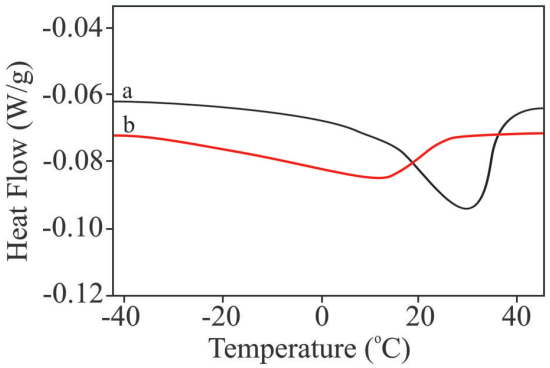

Fig. 5. DSC curve of nanocrystalline NiTi (a) and NiTi-2.5 wt.% HA nanocomposite (b) on heating

Fig. 5 shows DSC curves of NiTi-x wt.% HA nanocomposites (x=0, 2.5), where phase transformation peaks of 2.5 wt.% HA are weaker than that of pure NiTi. Only one phase transformation peak appears in NiTi-2.5 wt.% HA upon heating, which corresponds to one-step B2-B19' transformation. The difference in peak temperature of phase transformation between NiTi and 2.5 wt.% HA is about 15 °C. This is the result of the formation of several second-phases in the NiTi matrix. The second-phases have no phase transformation behavior whereas only the NiTi matrix does, leading to the peak temperature of phase transformation for 2.5 wt.% HA beings lightly different from that of pure NiTi. Factors that may influence the temperature of phase transformation of the NiTi alloy and NiTi-2.5 wt.% HA composite synthesized in the present work, except the other phases, may include oxygen and iron contamination from ball milling, too [8].

Recent studies showed clearly that nanostructuring of Ti-based biomaterials can considerably improve not only the mechanical properties, but also the biocompatibility [1, 9].

4. Conclusions

In this work, the mechanical alloying was used to synthesize nanostructured NiTi-x wt. % HA nanocomposites. This technique enables alloying of elements that are difficult or impossible to combine by conventional melting methods (i.e. NiTi and HA). NiTi based nanocomposite reinforced with HA particles were successfully fabricated by mechanical alloying and powder metallurgical process. Different phase constitutions have influence on the mechanical and corrosion properties of sintered materials. Vickers hardness change corresponding to the relative density. Introduction of HA particles leads to a change of phase constituents of the NiTi matrix, while slightly affecting its phase transformation characteristics.

TABLE 1

Mean values of corrosion current densities (I_C) and corrosion potentials (E_C) of studied bulk NiTi-HA type nanocomposites

	NiTi	NiTi-2.5 wt. HA	NiTi-5 wt.% HA	NiTi-5 wt.% HA
IC [A/cm^2]	2.5×10-7	2.6×10-6	3.2×10-6	5.2×10-5
EC [V]	-1.055	-0.677	-0.972	-1.262

REFERENCES

[1] L. Zhang, T.J. Webster, Nano Today **66**,4 (2009).

[2] M. Geetha, A.K. Singh, R. Asokamani, A.K. Gogia, Progr. Mater. Sci. **397**, 54 (2009).

[3] J.S. Benjamin, Sci. Am. **40**, 234 (1976).

[4] Z.G. Wei, R. Sandstrom, S. Miyazaki, J. Mater. Sci. **33**, 3743 (1998).

[5] D.J. Wever, A.G. Veldhuizen, M.M. Sanders, J.M. Schakenraad, J.R. Horn, Biomaterials **1115**, 18 (1997).

[6] K. Niespodziana, K. Jurczyk, J. Jakubowicz, M. Jurczyk, Mater. Chem. Phys. **160**, 123 (2010).

[7] H.J. Jiang, S.Cao, C.B.Ke, X.Ma, X.P. Zhang, Mater. Lett. **74**, 100 (2013).

[8] O.D. Neikov, S.S. Naboychenko, I.V. Murashova, V.G. Gopienko, I.V. Frishberg, D.V. Lotsko, Handbook of Non-Ferrous Metal Powders: Technologies and Applications, Elsevier 2009.

[9] M. Kaczmarek, M.U. Jurczyk, B. Rubis, A. Banaszak, A. Kolecka, A. Paszel, A. K. Jurczyk, M. Murias, J. Sikora, M. Jurczyk, M. J. Biomed. Mater. Res. **102A**, 1316 (2014).